Optical and Infrared Light Curves of the Eclipsing X-ray Binary V395 Car = 2S 0921–630

T. A. Ashcraft¹, R. I. Hynes², and E. L. Robinson³

- ¹School of Earth and Space Exploration, Arizona State University, Tempe, AZ 85287-1404, USA
- ²Department of Physics and Astronomy, Louisiana State University, Baton Rouge, Louisiana 70803, USA
- ³ Department of Astronomy, The University of Texas at Austin, 1 University Station C1400, Austin, Texas 78712, USA

In press

ABSTRACT

We present results of optical and infrared photometric monitoring of the eclipsing low-mass X-ray binary V395 Car (2S 0921–630). Our observations reveal a clear, repeating orbital modulation with an amplitude of about one magnitude in B, and V and a little less in J. Combining our data with archival observations spanning about 20 years, we derive an updated ephemeris with orbital period $9.0026 \pm 0.0001 \,\mathrm{d}$. We attribute the modulation to a combination of the changing aspect of the irradiated face of the companion star and eclipses of the accretion disk around the neutron star. Both appear to be necessary as a secondary eclipse of the companion star is clearly seen. We model the B, V, and J lightcurves using a simple model of an accretion disk and companion star and find a good fit is possible for binary inclinations of $82.2 \pm 1.0^{\circ}$. We estimate the irradiating luminosity to be about $8 \times 10^{35} \,\mathrm{erg \, s^{-1}}$, in good agreement with X-ray constraints.

Key words: accretion, accretion disks — binaries: close — binaries: eclipsing — stars: individual: V395 Car, 2S 0921-630

1 INTRODUCTION

2S 0921–630 was discovered as an X-ray source by Li et al. (1978) using SAS-3 and was identified with an approximate 17th magnitude star, V395 Car. The system shows partial eclipses in both the optical and X-ray bands (Branduardi-Raymont et al. 1983; Chevalier & Ilovaisky 1982; Mason et al. 1987). The orbital period is about 9 days and the system must have an inclination between 70° and 90°. Optical dips of up to 2 magnitudes deep (Krzeminski & Kubiak 1991) have been present in optical light curves of V395 Car, but no complete orbital lightcurve has yet been published. The companion star has been identified as a K0 III star (Shahbaz et al. 1999).

Several attempts have been made to constrain the system parameters of V395 Car using the photospheric absorption lines from the companion star, which are detectable in spite of the large contamination by disk flux (Shahbaz et al. 1999, 2004; Jonker et al. 2005; Shahbaz & Watson 2007; Steeghs & Jonker 2007). From measurements of the radial velocity curve and rotational broadening, and assuming an appropriate inclination for an eclipsing system, it is possible to solve for the masses of both objects. The remaining uncertainty is in the 'K-correction', which accounts for suppression of absorption lines on the inner face of the companion star by irradiation. Assuming negligible K-correction and an inclination of $i=83^{\circ}$, Steeghs & Jonker (2007) deduce a

compact object mass of $M_1 = 1.44 \pm 0.1 \,\mathrm{M}_\odot$, a companion star mass of $M_2 = 0.35 \pm 0.03 \,\mathrm{M}_\odot$, and hence a mass ratio of $q = 0.24 \pm 0.02$. Shahbaz & Watson (2007) assume $i = 75^\circ$ and deduce $M_1 = 1.37 \pm 0.13 \,\mathrm{M}_\odot$ and $q = 0.281 \pm 0.034$. We note that the assumed inclination does not affect the derived mass ratio, and that the two estimates of q are consistent. The mass estimates, too, agree, and both are consistent with a canonical mass neutron star, in contrast to earlier mass estimates (Shahbaz et al. 2004; Jonker et al. 2005), which used the overestimated rotational broadening measurement of Shahbaz et al. (1999).

Because V395 Car eclipses, the inclination is relatively well constrained and the derived parameters are relatively insensitive to the remaining inclination uncertainty. Nonetheless, it is still of interest to examine the orbital lightcurve of the binary, and in fact it is an advantage that the system parameters are already well constrained, reducing the uncertainty in the interpretation of the lightcurves.

In this paper we present optical and IR photometry from two observing seasons totalling 187 nights of monitoring of V395 Car obtained to investigate both the orbital and longer-term lightcurve. We begin by describing our data in Section 2. Section 3 presents the long-term lightcurve, and Section 4 proceeds to derive an improved measurement of the orbital period and ephemeris zero-point based on these data together with archival measurements. With the period

firmly established, we present orbital lightcurves in the three bands in Section 5 and model them in Section 6. We discuss the implications of our results in Section 7 and summarise our conclusions in Section 8.

OBSERVATIONS AND DATA REDUCTION

Optical and Infrared Data

Using the SMARTS 1.3 m telescope at Cerro Tololo Inter-American Observatory with the dual-channel optical/IR ANDICAM, images were taken almost daily from 2004 November through 2005 July and in 2005 December of V395 Car in the B, V, and J bands. For various reasons such as equipment and weather problems, there are a few long gaps in the data. The overall quality of the images was typically good, with seeing of 1-2 arcsec. Usable data were obtained on a total of 187 nights.

On each night two images were taken in the V band with $130 \,\mathrm{s}$ exposure time and two in the B band with a 100 s exposure time. Pipeline data reduction for the optical frames was done prior to receiving the images and appeared satisfactory, with no residual artifacts of poor bias corretion or flat-fielding. We show the central portion of the average V frame in Figure 1. Each night differential aperture photometry was performed relative to a bright reference star for the target and three other comparison stars used to check the stability using standard IRAF¹ routines.

Additionally, nine images with 50 s exposure time were taken each night in the J band, with each image shifted with respect to the others. The nine images were median combined in IRAF to create a sky image which was subtracted from each individual image before flat-fielding using dome flats. The reduced images were shifted and averaged to produce one final image per night.

LONG-TERM LIGHTCURVES

To obtain the lightcurves we performed differential photometry relative to a comparison star. The same comparison star was used for the B and V bands (C1 in Figure ??) but a different one was necessary for J, C2, as C1 was not consistently located in the smaller IR field of view. We show the combined long-term lightcurve in Figure 2. In this, and all plots in this paper, we show differential magnitudes relative to the comparison star used. The lightcurves in all the bands exhibit only the basic eclipsing binary modulation. There are no indications of any longterm variation in the out of eclipse lightcurve.

PERIOD ANALYSIS

For each band, B, V, and J, we computed the periodogram using the Lomb-Scargle technique to investigate the different possible periods. We show the V band periodogram in

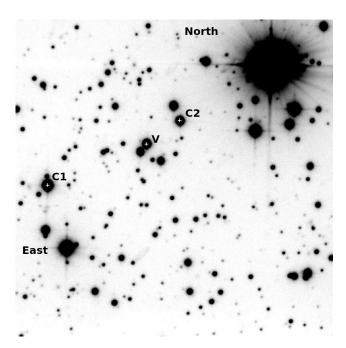


Figure 1. Finder chart based on the average of all of our Vband images. V395 Car is labeled V, the comparison star used for optical images is C1 and the IR comparison is C2. The field of view is 3 arcmin square.

Figure 3. Two strong peaks were seen, a strong fundamental near 9 days and a first harmonic. For the B and V bands peak at 9 days is dominant. The J band is more affected by the secondary eclipse, which caused the first harmonic to slightly dominate. We measured the fundamental periods to be $9.01307 \, \text{days}$ (B), $9.01632 \, \text{days}$ (V), and $9.02283 \, \text{days}$ (J). A period of 9.017 \pm 0.005 days came from averaging together the period from each filter. The accuracy of the period found from this method is not high because it is sensitive to slight changes in the data. Furthermore, since all of the filters were obtained at approximately the same time, they are not fully independent, and the uncertainty quoted is an underestimate. The mean period does agree with the periods others have previously found: $9.0035 \pm 0.0029 \,\mathrm{days}$ (Shahbaz et al. 2004) and 9.006 ± 0.007 days (Jonker et al. 2005).

We can obtain a much more precise measurement of the period by combining our data with previously published data. We measured the time of nine different mid-eclipses for which there were data available for three consecutive days around the time of mid-eclipse. Averaging these nine eclipses together, an ephemeris of eclipse of $T_0 = 2453397.52 \pm 0.08$ in HJD was determined. The uncertainty on this was large and we found that when we folded and fit the lightcurve in Section 6 a phase offset of -0.0271 ± 0.0024 was required. Correcting for this offset, we refine our eclipse ephemeris to $T_0 = 2453397.28 \pm 0.02$. Using the previously calculated time of mid-eclipse of 2446249.18 from the ephemeris of Mason et al. (1987) and the newly calculated one, and assuming that the Shahbaz et al. (2004) period (the most precise previously available) is accurate, a refined orbital period could be 8.9913 ± 0.0001 days (795 cycles), 9.0026 \pm 0.0001 days (794 cycles), or 9.0140 \pm 0.0001 days (793

¹ IRAF is distributed by the National Optical Astronomy Observatories, which are operated by the Association of Universities for Research in Astronomy, Inc., under cooperative agreement with the National Science Foundation.

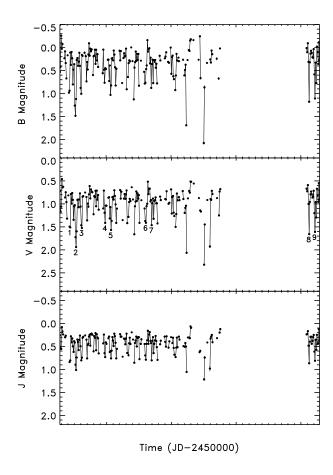


Figure 2. Plot of the long-term lightcurves in the B, V, and J bands. For the B and V bands the data points for the two images taken each night were averaged together for clarity. The dates of the 9 eclipses used to find the ephemeris are labelled 1-9.

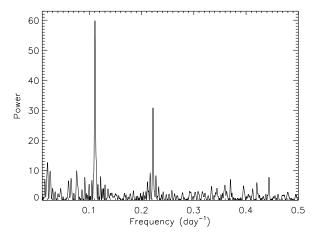


Figure 3. Periodogram of the V band. It only shows frequencies up to $0.5 \, \mathrm{day^{-1}}$ since higher ones are duplicates of their lower frequency counterpart. The peak of 9.01632 days clearly dominates over the peak caused by the secondary eclipse.

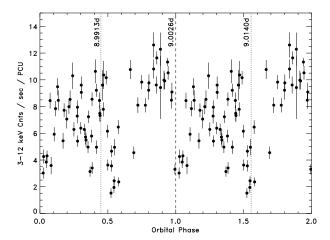


Figure 4. RXTE/PCA lightcurve from 1996 folded on the 9.0026 d period. The dashed lines indicate times of predicted eclipse for not only this period, but for the other two candidates. Since the X-ray observations were concentrated in a short period, the primary effect of different assumed orbital periods is to shift the minimum as indicated.

cycles), where only 9.0026 days is consistent within the uncertainties of Shahbaz at the 3σ level.

To attempt to confirm the identification of the correct alias, we also examined 75 archival Rossi X-ray Timing Explorer PCA observations obtained from April 12 to May 2, 1996. We extracted 3–12 keV background subtracted fluxes from Standard 2 data and combined each ($\sim 1000\,\mathrm{s}$) exposure into a single average point. We show these data folded on the 9.0026 d period in Figure 4; folding on the alternative periods results in lightcurves that are just shifted, so rather than replicate the data we show where phase zero is predicted to fall for each of these periods.

2S 0921–630 is known to show X-ray eclipses at phase zero (Branduardi-Raymont et al. 1983). From the X-ray lightcurve we can therefore rule out the period of 8.9913 days since no structure is seen at phase 0. The 9.0026 d period does produce an apparent eclipse centred at phase zero as expected. However the 9.0140 d period also produces a minimum at around the same phase, albeit a less uniform one. The X-ray eclipse presented by Mason et al. (1987) has a full width of ~ 0.15 in orbital phase, and drops to about 25 percent of the peak intensity. This is a rather good match to the eclipse width and depth we obtain from a 9.0026 day period supporting that identification. If this is correct, then there is a broad and irregular dipping structure from phase 0.5–0.7 which would be consistent with X-ray dipping seen in other high inclination LMXBs. While we cannot absolutely rule out a 9.0140 d period, we conclude that 9.0026 d is most likely to be the true orbital period (consistent with the measurement of Shahbaz et al. 2004), and so derive an updated ephemeris:

$$T_0(\text{HJD}) = 2453397.28(2) + 9.0026(1)E$$

where T_0 is the time of ecclipse. We note that the difference between the 9.0026 day and 9.0140 day period has negligible effect on the folding of our lightcurves and so does not affect the subsequent analysis or modeling.

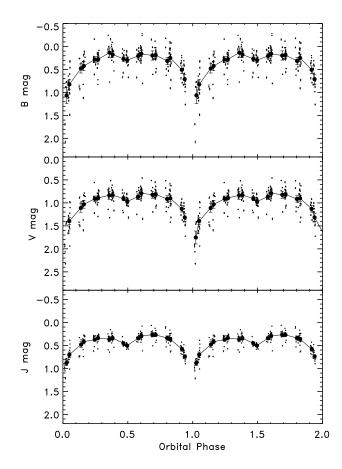


Figure 5. Orbital lightcurves of V395 Car in all three bands B, V, and J created by folding the data over a period of 9.0026 days. Larger points are phase-binned averages and are joined by lines for clarity.

5 ORBITAL LIGHTCURVES

Fig. 5 shows the orbital lightcurve based on our ephemeris. Since the period is almost a whole number of days the points are bunched up in phase leading to incomplete coverage, especially during primary eclipse.

Each band clearly shows a primary deep eclipse and shallower secondary eclipse with the primary eclipse having the greatest depth in the B band and the secondary being the most prominent in the infrared J band. The depths of the primary eclipse are ~ 2.5 mag in B, ~ 1.9 mag in V, and ~ 1.1 mag in J.

6 MODELLING LIGHTCURVES

We modelled the lightcurves using the XRbinary² code, version 2.1. This code has previously been used for the LMXBs UW CrB (Mason et al. 2008), 4U 1822–371 (Bayless et al. 2010), and 4U 1957+115 (Bayless et al. 2011), as well as for the cataclysmic variable SS Cyg (Bitner, Robinson, & Behr

2007). The general approach is to model the disk and companion star as a series of tiles. Irradiation is calculated by ray-tracing, allowing for rather complex disk geometries. For this analysis, we have used only the simplest symmetric disk model, which nonetheless provides quite a good fit to the multi-band data.

The system parameters of V395 Car are relatively well known, at least compared to many neutron star LMXBs. The mass ratio, independent of inclination, has been independently estimated at $q=0.281\pm0.034$ (Shahbaz & Watson 2007), and $q=0.24\pm0.02$ (Steeghs & Jonker 2007). Both groups used essentially the same method, measuring the radial velocity semi-amplitude and rotational broadening of the companion star and deducing the mass ratio using the relationship of Wade & Horne (1988). We adopt q=0.26 for this analysis as an average of the two measurements. Steeghs & Jonker (2007) noted that for their mass ratio, the X-ray eclipse observation of Mason et al. (1987) implies an inclination about $i=83^{\circ}$, but we will leave the inclination as a free parameter when modelling the lightcurves.

We assume illumination of the disk and companion star by a source of X-rays at a height above the accretion disk intended to mimic an accretion disk corona (ADC). The X-ray source is specified by its luminosity and the height above and below the plane (it is treated as a lamppost). In the limit of placing this at a negligible height above the accretion disk, this also would represent central illumination from the neutron star. We also experimented with models in which the accretion disk was simply given a parameterised temperature distribution, $T \propto R^{-0.5}$ or $T \propto R^{-0.75}$, but found these produced inferior fits compared to the lamppost ADC model.

For the disk geometry, we assume a thin, flared, axisymmetric disk, with $H/R \propto R^{1.21}$, where H is the local disk height and R is the radius. The height and radius of the outer edge of the disk are free parameters. We adopted an exponent of 1.21 as representative of values proposed in the literature rather than strongly motivated in its own right, but we also repeated the analysis with $H/R \propto R^{1.10}$ and $H/R \propto R^{1.29}$ and found negligible difference, and in particular no effect on the preferred inclination. This is expected as our fits preferred a very thin disk and a significantly elevated X-ray source. With these parameters the shape of the disk has relatively little effect and irradiation is possible even if the real disk profile is convex (Dubus et al. 1999). The outer radius of the disk is a free parameter but since the outer radius is limited by tidal truncation, we constrain it to be less than $0.9 R_{\text{lobe}}$ (Whitehurst & King 1991).

Reprocessing of X-rays will also be affected by a local albedo. We assume all X-rays incident on the companion are reprocessed, but that a fraction of those incident on the disk might be Compton reflected, with the fraction left as a free parameter. While some Compton reflection from the companion star is also possible, we fold this uncertainty into the X-ray luminosity, as there are really only two independent parameters that can be constrained here: the heating of the disk and the heating of the donor star. The assumption being made is that the accretion disk will be more highly ionised than the companion star, and irradiated predominantly at a steeper angle of incidence, so would be expected

² A full description of the program is available at http://pisces.as.utexas.edu/robinson/XRbinary.pdf.

to thermally reprocess a smaller fraction of X-rays than the donor star.

To summarise this discussion, the free parameters of the model are the binary inclination (i), the disk outer radius (R_{out}) and height (H_{out}) , the X-ray luminosity (L_{X}) , the height of the X-ray source above the plane (H_{ADC}) , and the relative albedo of the disk and donor star. We performed a series of fits with fixed trial inclinations, as this is the parameter which we care most about, while leaving other parameters free to vary (subject to constraints on the disk radius and relative albedo). All fits were begun using a downhill simplex (amoeba) algorithm. Multiple starting simplexes were tested, and each fit was refined using Powell's method.

We fitted models at 0.1° intervals from $80\text{--}85^{\circ}$, and more coarsely beyond that. We find a best fitting value of $i=82.2\pm1.0^{\circ}$ (1σ). We also ran fits for q=0.24 and q=0.28. These were minimally different, with the best fitting inclination shifted by no more than 0.2° , a difference negligible compared to our statistical uncertainty. The best-fitting model is shown in Fig. 6. It corresponds to $i=82.2^{\circ}$, $L_{\rm X}=8\times10^{35}\,{\rm erg\,s^{-1}}$, $R_{\rm disk}=0.89R_{\rm lobe}$, H/R=0.001, $H_{ADC}=0.16a$, and equal disk and donor star albedos. It is apparent that the deepest points of the model primary eclipse are much deeper than the binned points, especially at shorter wavelengths. This is a consequence of the sampling however, and examining Fig. 5, we can see that the same trend is present in the unbinned data.

7 DISCUSSION

The inclination we derive is consistent with previous estimates. For example, Steeghs & Jonker (2007) comment that for their mass ratio, an inclination of 83° is implied by the X-ray lightcurve of Mason et al. (1987). Consequently, our inclination does not change current estimates of the neutron star mass significantly, especially as the derived mass is relatively insensitive to inclination for high inclinations. Nonetheless, pinning down the inclination does increase the confidence in this measurement. Steeghs & Jonker (2007) estimated $M_1 = 1.44 \pm 0.10 \, \mathrm{M}_{\odot}$ by assuming i = 83.0 with no uncertainty in inclination. Adopting instead $i = 82.2 \pm 1.0^{\circ}$ and performing a similar Monte-Carlo simulation to that used by the authors does not change either the derived value or its uncertainty.

While our estimate of the luminosity of the X-ray source is indirect, it is consistent with (and independent of) that of Kallman et al. (2003); $L_{\rm X} < 10^{36}~{\rm erg\,s^{-1}}$ for cases in which we see the full X-ray luminosity. The luminosity sensitivity of our lightcurve fitting arises because the X-ray luminosity sets the temperatures of the accretion disk and companion star. Different temperatures will change the relative depths of primary and secondary eclipses as a function of bandpass, so the broad wavelength coverage of our data is what leads to our sensitivity to the X-ray luminosity. Our measurement is very model dependent and cannot be a precise one, but is consistent with the model of Kallman et al. (2003) in which we see the full X-ray luminosity rather than a small fraction of it as in canonical ADC sources.

Of the other parameters, the disk radius implies a tidally truncated disk, as might be expected. The disk thickness is smaller than would typically be expected, but may

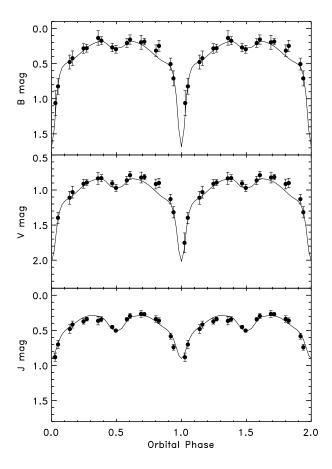


Figure 6. The orbital binned lightcurve fitted with the best-fitting solution.

simply indicate that the disk thickness is negligible compared to the vertical extent of the X-ray emitting region, which we infer to be rather large. A large X-ray emitting region is also required by the presence of partial eclipses at X-ray wavelengths, so is not surprising.

Finally, we note that there is a small residual asymmetry in the lightcurves. This is common in LMXBs and usually attributed to non-axisymmetric structure in the accretion disk. Given that it is a small effect and that our lightcurves are not well sampled we do not try to model the asymmetry numerically.

8 CONCLUSIONS

We have obtained the first full, and multi-colour, orbital light curve of the long-period LMXB V395 Car. We refine the orbital period to $9.0026\pm0.0001\,\mathrm{days}$ and present an updated time of minimum, $T_0=2453397.28\pm0.02$ (HJD). We successfully fit our BVJ lightcurves using the XRbinary code and derive a binary inclination of $i=82.2\pm1.0^\circ$. This is consistent with previous constraints and does not change previously published compact object mass estimates.

We also estimate an X-ray luminosity of $10^{36} \, \mathrm{erg \, s}^{-1}$, consistent with X-ray estimates of Kallman et al. (2003). This makes V395 Car a relatively low mass-transfer rate system in sharp contrast to 4U 1822–371 where an accretion

rate close to the Eddington limit is inferred. (Bayless et al. 2010).

With the period so close to an integer days, one of the major limitations of our dataset remains the incomplete sampling in orbital phase. Further progress will require a completely sampled lightcurve, and consequently a multisite campaign spanning a range of longitudes.

ACKNOWLEDGMENTS

This work uses data obtained on the 1.3 m telescope at Cerro Tololo Inter-American Observatory which is operated by the SMARTS Consortium. This research has made use of data obtained through the High Energy Astrophysics Science Archive Research Center Online Service, provided by the NASA/Goddard Space Flight Center and has also made use of the NASA ADS Abstract Service. R.I.H. acknowledges support from NASA/Louisiana Board of Regents grant NNX07AT62A/LEQSF(2007-10) Phase3-02 and National Science Foundation Grant No. AST-0908789.

REFERENCES

Bayless A. J., Robinson E. L., Hynes R. I., Ashcraft T. A., Cornell M. E., 2010, ApJ, 709, 251

Bayless A. J., Robinson E. L., Mason P. A., Robertson P. 2011, ApJ, 730, 43

Bitner M. A., Robinson E. L., Behr B. B., 2007, ApJ, 662, 564

Branduardi-Raymont, G., Corbet, R. H. D., Mason, K. O., Parmar, A. N., Murdin, P. G., & White, N. E. 1983, MN-RAS, 205, 403

Chevalier, C., & Ilovaisky, S. A. 1982, A&A, 112, 68

Dubus G., Lasota J.-P., Hameury J.-M., Charles P., 1999, MNRAS, 303, 139

Jonker, P.G., Steeghs, D., Nelemans, G., & van der Klis, M., 2005, MNRAS, 356, 621

Kallman, T. R., Angelini, L., Boroson, B., & Cottam, J. 2003, ApJ, 583, 861

Krzeminski, W., & Kubiak, M., 1991, Acta Astronomica, 41, 117

Li, F.K., Clark, G.W., Jernigan, J.G., Laustsen, S., Zuiderwijk, E., & van Paradijs, J.A., 1978, Nat, 276, 799

Mason, K.O., Branduardi-Raymont, G., Codova, F.A., & Corbet, R.H.D., 1987, MNRAS, 226, 423

Mason P. A., Robinson E. L., Gray C. L., Hynes R. I., 2008, ApJ, 685, 428

Shahbaz, T., Kuulkers, E., Charles, P.A., van der Hooft, F., Casares, J., & van Paradijs, J., 1999, A&A, 344, 101

Shahbaz, T., Casares, J., Watson, C.A., Charles, P.A., Hynes, R.I., Shih, S.C., & Steeghs, D., 2005, ApJ, 616, L123

Shahbaz T., Watson C. A., 2007, A&A, 474, 969

Steeghs D., Jonker P. G., 2007, ApJ, 669, L85

Wade R. A., Horne K., 1988, ApJ, 324, 411

Whitehurst R., King A., 1991, MNRAS, 249, 25